Genome-Wide Identification of The NHXs in Rosa Multiflora Reveals a Key Role of RmNHX2 in Salt Tolerance

Luo Ping (pingluo@zafu.edu.cn)
Zhejiang A and F University
Yuxiao Shen
Henan Agricultural University
Linmei Chen
Zhejiang Agriculture and Forestry University: Zhejiang A and F University
Wen Chen
Zhejiang Agriculture and Forestry University: Zhejiang A and F University
Yongyi Cui
Zhejiang Agriculture and Forestry University: Zhejiang A and F University

Research Article

Keywords: Rosa multiflora, RmNHX2, salt tolerance, ion homeostasis, ROS scavenging

Posted Date: October 22nd, 2021

DOI: https://doi.org/10.21203/rs.3.rs-938972/v1

Abstract

High salinity restricts plant growth and geographic distribution. Plant intracellular Na^+/H^+ (NHX) antiporters have critical roles in plant development and stress response. However, the molecular functions of *RmNHXs* in *Rosa multiflora* remain obscure. In this study, we identified 11 putative *RmNHXs* in *Rosa multiflora* according to the genome-wide analysis. The *RmNHX* genes were classified into 3 classes. Most of the *RmNHX* genes were responsive to salt stress, with the greatest up-regulation being observed in *RmNHX2*. *RmNHX2* was localized at the tonoplast. *RmNHX2* overexpression resulted in the enhanced salt tolerance in tobacco, whereas virus-induced gene silencing (VIGS) of *RmNHX2 in R.multiflora* increasedsalt susceptibility. Under salt treatment, the transgenic tobacco plants achieved less reactive oxygen species (ROS) accumulation and higher activities of enzymes (e.g., superoxide dismutase (SOD), peroxidase (POD) and catalase (CAT)), which complied with the up-regulated expressions of antioxidant genes. In addition, *RmNHX2*-overexpression lines had a lower level of Na^+, a higher level of K^+, as well as a lower Na/K ratio. In contrast to the mentioned, VIGS of *RmNHX2 in R.multiflora* exhibited the opposite phenotype, accompanied by compromised salt tolerance. *RmNHX2* enhances plant salt tolerance by maintaining proper ion homeostasis, as well as by accelerating ROS scavenging. For this reason, *RmNHX2* has great potential to be employed for the engineering of ornamental plants in terms of enhanced salt tolerance subsequently.

Introduction

Abiotic stresses involve the environment conditions (e.g., salt injury, extreme temperature and drought) severely affecting the quantity and quality of crop product. Salt stress refers to a major stress depressing plant growing process and limit crop production, and has been a great threat to agricultural development all over the world (Mahajan and Tuteja. 2005). Moreover, fertilization and irrigation could cause secondary soil salinity (Zhu 2002). In addition, salinity can destroy physio-biochemical function and cause the death of plant cells and plant itself via osmotic stress, ion toxicity and nutrition imbalance attributed to excess of Na^+ and Cl^- (Kronzucker et al. 2011). Accordingly, analyzing the mechanism underlying plants responses to salt stress, exploring salt tolerance related genes can theoretically and practically help.

To address soil salinity, plants have developed several adaptive mechanisms that are crucial for their survival of many plants (Yoshida et al. 2014). Plants are capable of perceiving the salt stress signals from their cellular, physiological and biochemical responses, transmitting the signals as well as regulating expression of related genes to respond to salinity (Giraud et al. 2009). For instance, plants could control the loss of water to alleviate salt damage via regulating the closure of the stomata (Zhang et al. 2019). Over the past few decades, it was extensively demonstrated that salt tolerant related genes could fall to two groups in accordance with their products' function. The former group's function is protecting cell against damage derived from salt stress (Phukan et al. 2017). Transcription factors (TFs), protein phosphatases and protein kinases, i.e., the second group, are critical to stress signal transduction and stress-responsive gene activation (Yu et al. 2017). As genetic engineering leaps forward, horticultural

crops can be advanced at the gene level and increase the resistance ability (Dong et al. 2013). Furthermore, given that, it will be of high significance for exploiting the favorable genes to increase the salt tolerance of plants.

Plants have evolved several defense systems (e.g., ion efflux from cells and sequestration) to adapt to the salt stress (Banjara et al. 2012). The plant sodium-proton antiporters (NHXs) were demonstrated initially to have a mediating effect on the electroneutral Na^+/H^+ exchanging process, sequestering excess cytosolic Na^+ to the vacuole and maintaining ionic equilibrium (Yuan et al. 2015). It was reported that there are eight NHX members in *Arabidopsis* (Deinlein et al. 2014). According to the sequence similarity and localization, the NHXs of *Arabidopsis* fall to three distinct classes, i.e., the plasma membrane-located AtNHX7/8, endosome-located AtNHX5/6 and vacuolar membrane-located AtNHX1/2/3/4 (Bassil and Blumwald, 2014). It is noteworthy that the vacuolar and plasma membrane-located NHXs in *Arabidopsis* critically impact the salt tolerance through the maintenance of Na^+/K^+ homeostasis (Bassil et al. 2011). Recent studies suggested that overexpression of the mentioned vacuolar Na^+/H^+ antiporters led to the increased salt tolerance in several plant species (Qiao et al. 2007, Teakle et al. 2010, Zhang et al. 2015). For instance, heterologous expression of two NHXs (*HtNHX1* and *HtNHX2*) from a salt-tolerant plant *Helianthus tuberosus* increased the salt tolerance of rice (Zen et al. 2018). In *Pyrus ussuriensis*, the overexpression of *PbrNHX2*, located in the tonoplast, enhanced salt tolerance by maintaining a high K^+/Na^+ ratio (Dong et al. 2019). The mentioned results indicated that NHXs proteins positively impacted plant salt tolerance. It is critical to isolate and characterize the function of NHXs in plants.

Rosa multiflora Thunb as root stock for modern rose (*Rosa hybrida*) is a cold and salt tolerant genotype; thus, the functional identification of salt-tolerant genes would substantially benefit genetic breeding of roses. This study characterized *RmNHX2* from *Rosa multiflora*. *RmNHX2* overexpression in tobacco increased the salt tolerance, whereas down-regulation of *RmNHX2* in *Rosa multiflora* by VIGS led to the improved salt sensitivity as well. As revealed from the results here, the *RmNHX2* gene could potentially be employed in the improvement of subsequent rose salt tolerance.

Materials And Methods

Identification of the *NHX* family genes in *Rosa multiflora*

The annotated protein sequences of *Rosa multiflora* were downloaded from *R.multiflora* Genome database (http://kazusa.or.jp/index.html). The Hidden Markov Model (HMM) file corresponding to the Na^+/H^+ exchanger domain (PF00999) was downloaded from the Pfam protein family database (http://pfam.xfam.org/). TBtools was employed to obtain the putative RmNHXs in *Rosa multiflora* (*E-value*$<1e^{-5}$) (Chen et al. 2020). The existence of the conserved Na^+/H^+ exchanger domain was examined using the SMART (http://smart.emblheidelberg.de/) and NCBI-CDD search (http://www.ncbi.nlm.nih.gov/Structure/cdd/wrpsb.cgi). Sequences without the Na^+/H^+ exchanger domain were excluded. The online programs Expasy (http://web.expasy.org/compute_pi/) was used to predict the molecular weight (Mw) and isoelectric point (pI) of the putative RmNHXs. According to the

conserved domains of NHXs in wild rose, rosa, strawberry, apple, cherry, raspberry and *Arabidopsis*, a phylogenetic tree was constructed in MEGA7.0 with Neighbor-Joining method (bootstrap = 1000).

Gene structure, conserved motif and promoter analyses

Gene Structure Display Server（http://gsds.cbi.pku.edu.cn/）was employed for intron and exon analysis. The conserved motifs in the protein sequences were examined with Pfam. The cis-acting elements in the promoters (up to 2000-bp upstream ATG) of the *RmNHXs* genes were analyzed by PlantCARE (http://bioinformatics.psb.ugent.be/webtools/plantcare/html).

Plant material and stress treatment

Seeds of *Rosa multiflora* were collected in the Zhejiang A&F University Rose Germplasm Resources. The seeds stored in humid sand were maintained at the temperature of 4 °C. After 2 months, the seeds were transferred into plugs in artificial climate box of 16 h light/8 h dark cycles at 22 °C. 60-day-old *Rosa multiflora* seedlings underwent the exposure to the stress treatment to analyze the *RmNHXs* expression pattern. For salt treatment, each seedling was sprayed with 50 mL of 200 mM NaCl solution and sampled after 1, 5, 12, 24, and 48 h in a growing chamber. At least 40 uniform seedlings were employed for salt stress treatment. Leaves were harvested from 4 seedlings harvested in a random manner under the set points of respective treating process and blended as a pool of sample materials. Leaf samples were promptly frozen in liquid nitrogen and then stored in -80 °C till their utilization.

RNA extracting process and quantitative real-time PCR study (qRT-PCR)

By using Easyspin Plant RNA Kit (Aidlab, Beijing, China) following the instructions for use, total RNA was extracted from the samples. Subsequently, 1 μg of total RNA was reversely transcribed to cDNA by using PrimeScript RT Reagent Kit With gDNA Eraser (TaKaRa, Dalian, China). Based on a 7500 real-time PCR cycler (Applied Biosystems, CA, USA) and the SYBR Premix Ex Based on (TaKaRa, Dalian, China), qRT-PCR was performed. Supplementary Table 2 lists the sequences of primers. This study determined the relative expression level of target genes by using the $2^{-\Delta\Delta Ct}$ method (Kenneth and Livak, 2001). For *Rosa multiflora*, *RmGAPDH* was used as the internal control, and *NtEF1* was used as reference gene in tobacco. The expression level of each time point was detected at least three times, and the data are expressed as the mean values ± SE.

Isolation of *RmNHX2* and sequence analysis

The *RmNHX2* coding sequence was amplified with high fidelity Ex Taq (TaKaRa, Dalian, China) using gene-specific primers (Supplementary Table 2); next, the ligation into pMD 18-T vector (TaKaRa, Dalian, China) was conducted. It was confirmed by sequencing (TsingKe, Hangzhou, China). Based on ClustalW, several sequence alignments were conducted and presented by GeneDoc Software.

Subcellular localizing process of RmNHX2

To achieve the subcellular localization, the *RmNHX2* coding sequence without the stop codon was amplified by using specific primers (Supplementary Table 2), and then it was cloned into the pHBT-GFP-NOS vector at *BamH*I and *Sal*I restriction sites as promoted by the CaMV *35S*. The isolation of *Arabidopsis* protoplasts was conducted in line with the existing studies (Bai et al., 2014). *RmNHX2*-GFP plasmid was transiently expressed in the *Arabidopsis* protoplasts, as has been described previously (Ma et al., 2019). 10 μg of *RmNHX2*-GFP plasmid was gently mixed with 100 μL of the *Arabidopsis* protoplasts (10^5/mL), and the mixture was incubated at 23 °C for 12 h. Under laser scanning microscope (LSM410, Carl Zeiss), the green and red fluorescence signals in *Arabidopsis* protoplasts were detected.

Generation of *RmNHX2*-overexpressing tobacco lines

The CDS region of *RmNHX2* was amplified from pMD 18-T-*RmNHX2* vector by using specific primers (Supplementary Table 2) that contained *BamH*I and *Sal*I restriction sites and ligated into the identical sites of the expression vector pCAMBIA2300s, which was controlled by the CaMV *35S*. Based on the freeze-thaw method, the resulting plasmid was transformed to *A. tumefaciens* strain (EHA105). Tobacco (*Nicotiana tabacum* cv.'Xianzi') genetic transformation was conducted by complying with the existing study (Li et al., 2019). Besides, the molecular identification of regenerated plants was confirmed based on PCR by using two pairs of specific primers (Supplementary Table 2). By RT-PCR, this study determined the *RmNHX2* expression levels in the positive transgenic tobacco lines were determined. To perform the subsequent experiments, the T2 seeds of transgenic tobacco lines were adopted.

Generation of *RmNHX2* silenced plants by Virus-induced gene silencing (VIGS)

Following the previous study (Khaskheli et al. 2018) , virus-induced gene silencing (VIGS)-mediated suppression of *RmNHX2* was conducted. Here, based on PCR with specific primers, the *RmNHX2* ORF (52-531 bp)'s 487 bp fragment was obtained from pMD 18-T-*RmNHX2* vector (Supplementary Table 2). The PCR product was inserted into *Xba* I and *Sac* I locations of pTRV2 to produce pTRV2-*RmNHX2*. The pTRV1, pTRV2 and pTRV2-*RmNHX2* vectors were added to *A. tumefaciens* strain (GV3101) by freeze-thaw method. The VIGS-mediated suppression of *RmNHX* in *Rosa multiflora* was performed as described with minor modification (Tian et al., 2014). The bacterial cells (OD600 =1.0) supplemented by pTRV1 were mixed with pTRV2-*RmNHX2* or pTRV2 at 1:1 (v/v) in infiltration buffer (10 mM $MgCl_2$, 150 mM acetosyringone and 10 mM MES, pH 5.6) and maintained under darkness for 3 h under ambient temperature. *Rosa multiflora* seeds with emerging shoots (c. 1 cm long) were immersed into the bacterial mixtures and infiltration was conducted under vacuum at -25 kPa for twice, maintaining for 60 s. When the vacuum was released, the seeds were cleaned with distilled water and then planted in pots. Plants were grown in a growing chamber at 16 h light/8 h dark cycles at 22 °C, 70% relative humidity. After 10 d, the gene silencing efficiency was determined by qRT-PCR.

Salt stress tolerance assay

A series of experiments were designed to elucidate the function of *RmNHX2 in response to salt stress. First, leaves detached from 40 d transgenic and WT tobacco (WTt) plants were exposed to 200 mM NaCl*

for 24 h. Electrolyte leakage (EL) and malondialdehyde (MDA) contents of the treated leaves were measured at the end of stress treatment. Second, 30 d potted RmNHX2 overexpressing lines and control tobacco plants (WTt) were sprayed with 200 mM NaCl at 3 d intervals for 2 weeks. Moreover, *Rosa multiflora* 15 d *RmNHX2*-silenced (VIGS) and *Rosa multiflora* (WTr) plantlets were hydroponically grown for 7 d in 300 mM NaCl solution. In another experiment, *Rosa multiflora* 30 d VIGS potted plants was sprayed with 200 ml of 300 mM NaCl at 3 d intervals for 2 weeks. The respective treatment was repeated three times with consistent results. The physiological, biochemical and gene expression were performed after salt stress.

Physiological analyses

EL was determined as previously described (Dahro et al. 2016) . Besides, MDA, H_2O_2, O_2^- contents and antioxidant enzymes activities (i.e., CAT (EC 1.11.1.6), SOD (EC 1.15.1.1) and POD (EC 1.11.1.7) were also assayed with specific detection kits (Nanjing Jiancheng Bioengineering Institute, Nanjing, China) by complying with the manufacturer's protocol. Furthermore, total chlorophyll in the leaves was extracted and determined according to the method of Liu et al (2008). Na^+ and K^+ levels were determined under atomic absorption spectrophotometry with a previously described method (Zhang et al. 2017) . In brief, the dry samples of leaves and roots were ground into powder. Approximately, 0.1 g of tissue powder was dissolved with 5 ml deionized distilled water, followed by boiling in water bath for 2 h. Lastly, the extract was filtered, and then Na^+ and K^+ of the samples were measured.

In situ histochemical staining of ROS

The H_2O_2 and O_2^- accumulations in the samples were stained with 3,3' diaminobenzidine (DAB) and nitro blue tetrazolium (NBT), respectively (Wu et al. 2016; Luo et al., 2020) . In summary, the leaves were immersed in 1 mg ml^{-1} DAB (in 50 mM potassium phosphate, pH 3.8) fresh solution or NBT (in 50 mM potassium phosphate, pH 7.8) for 12 h in the dark at ambient temperature. The above stained leaves were immersed in 100 % ethanol until the chlorophyll faded and subsequently maintained in 70 % ethanol until being photographed.

Statistical analysis

Salt treatment was repeated at least two times with consistent results achieved. The representative one was presented, shown as mean ± SE. The data were processed with analysis of variance (ANOVA) using SAS software (SAS Institute, Cary, NC, USA). By conducting LSD' multiple range test, statistical differences were determined at the significance level of $P < 0.05$ (*), $P < 0.01$ (**) and $P < 0.001$ (***).

Results

Identification of *RmNHXs* in *Rosa multiflora*

A total of 11 NHXs in *Rosa multiflora* was obtained according to the genome-wide analysis (Fig. 1a). The basic parameters about these RmNHXs were exhibited in Supplementary Table 1, including gene ID, CDS length, molecular weight (Mw) and isoelectric point (pI). As presented in Supplementary Table 1, the RmNHXs proteins varied from 268 to 695 aa in size with pI being between 5.03-9.03 and MW being between 29.47-62.51 kD. In addition, the phylogenetic analysis was performed based on the RmNHXs and NHXs from other plant species, which could be classified as vacuolar (Class I), endosomal (Class II), and plasma membrane types (Class □) (Fig. 1b). Nine RmNHXs were categorized in Class I, one in Class II and one in Class □, respectively (Fig. 1b).

The intron-exon structure analysis was conducted in the conserved Na^+/H^+ exchanger domains of the *RmNHXs* genes (Fig. 2a). As shown in Fig. 2a, the gene structure of 11 *RmNHXs* showed diverse intron-exon patterns with the number of introns ranging from 7 to 24. On the other hand, the longest intron of *RmNHX2* is 2.9 kb. As a result, the genome sequences of *RmNHX2* reached 7.8 kb (Fig. 2b). These data revealed that the changes of the gene structure in *RmNHXs* might lead to their function divergences during the evolution.

To gain insights into the function of *RmNHXs*, the 2.0 kb promoter region of the *RmNHXs* was adopted to identify the cis-acting elements using PlantCARE database. According to Supplementary Fig. 1, the promoter region of *RmNHXs* had various cis-acting elements (e.g., CAAT-box, CCAAT-box, and TATA-box), thereby demonstrating that the *RmNHXs* are closely related to the plant growth and development. Moreover, plant hormone-responsive and stress-responsive elements were also identified in the promoter region of *RmNHXs*, including salicylic acid responsive elements (TCA-elements), auxin responsive elements (TGA-elements), MeJA-responsive elements (CGTCA-motif, TGACG-motif), ABA responsive elements (ABREs), gibberellinresponsive elements (TATC-box), low-temperature responsive elements (LTR), defense and stress responsiveness elements (TC-rich repeats) (Supplementary Fig. 1). It should be noticed that there were different number of hormone and stress response motif in the promoter region of *RmNHXs* (Fig. 2c). These results indicated that *RmNHXs* might have different role in hormone and stress response.

Expression pattern of *RmNHXs* in *Rosa multiflora*

To further explore the potential functions of *RmNHXs*, we conducted qRT-PCR to assess the expression pattern of *RmNHXs* in response to salt stress. When subjected to salt stress, most of *RmNHXs* showed alteration of expression levels, while the expression pattern of each *RmNHXs* were different, demonstrating differences in the potential roles of *RmNHXs* under salt response (Fig. 3a). Among them, the expression level of *RmNHX2* was drastically up-regulated by the salt treatment (Fig. 3a). *RmNHX2* expression efficiently increased in 0.5 h in response to salt stress, and it reached the maximum expression in 5 h (about 6.8-fold), followed by gradually declining until last time point (48 h) (Fig. 3a).

As shown in Fig. 3b, *RmNHX2* expression efficiently increased in 0.5 h in response to dehydration, after which it began to decline. When subjected to cold stress, the expressing state of *RmNHX2* did not

noticeably change, suggesting that *RmNHX2* was not cold-inducible (Fig. 3b). In the case of exogenous ABA treatment, *RmNHX2* mRNAs initially remained steady in 1h, and then elevated by 2.2-fold at 12 h (Fig. 3b). Compared with dehydration and ABA, the salt treatment caused a greater induction, indicating that *RmNHX2* might impact plant abiotic stresses resistance, especially salt. The *RmNHX2* was chosen for further function analysis.

Analysis of RmNHX2 protein sequence and its subcellular localization

The coding sequence of *RmNHX2* was 1632 bp, encoding a 543 amino acids protein. *RmNHX2* was deposited in GenBank with accession number MW358917. As revealed from multiple sequence alignment, RmNHX2 shared 12 conserved transmembrane domains highly consistent with FvNHX2 (94.11 %) (Fig. 3c). Motif scanning suggested that the amiloride binding site (87-LFFIYLLPPI-96) existed in the N-terminal of RmNHX2 (Fig. 3c). The structure and function of plant NHXs were closely related to their subcellular locations.

To determine putative role of *RmNHX2 in Rosa multiflora*, its ORF without stop codon was inserted into pHBT-GFP-NOS vector as driven by CaMV *35S*. In addition, the tonoplast marker protein VAC-RK was fused to C-terminal RFP. The mentioned plasmids were co-transformed into *Arabidopsis* protoplast cells. As demonstrated from transient expression assays, RmNHX2-GFP fluorescence perfectly overlapped with VAC-RK-RFP fluorescent signals (Fig. 3d). The mentioned results suggested that RmNHX2 was localized at the tonoplast.

RmNHX2 overexpression in tobacco led to enhanced salt tolerance

As *RmNHX2* expression was strongly up-regulated by salt, this study speculated that *RmNHX2* might perform important functions against salt stress. To test the role of *RmNHX2 in salt tolerance in depth, tobacco transgenic plants were generated through the leaf culture dish transformation. Totally, twelve positive transgenic lines were identified by genomic PCR analysis (Supplementary Fig. 3). And three RmNHX2* overexpressing (hereafter designated as OE1, OE7 and OE9, Supplementary Fig. 3) with higher expressing levels of *RmNHX2* were chosen for further experiment. To determine whether *RmNHX2* overexpression led to the increased salt stress resistance of the transgenic plants, the fully expanded leaves detached from 40-day-old *RmNHX2*-overexpresing lines and wild type tobacco (WTt) were administrated with 200 mM NaCl for 24 h. Before salt treatment, WTt and transgenic tobacco lines did not show any noticeable difference in morphology. However, the WTt leaves showed serious wilting as compared with the transgenic tobacco lines after incubation in 200 mM salt solution (Fig. 4a). Electrolyte leakage (EL) and malondialdehyde (MDA) as a vital indicator of cell damage was measured after salt stress between transgenic lines and WTt (Wang et al., 2019). EL of the transgenic lines (25.7 % for OE1, 34.5 % for OE7 and 37.1 % for OE9) were significantly lower than 52.7 % of WTt (Fig. 4b). According to Fig. 4c, the MDA level was prominently lower in the transgenic lines than in WTt after the salt stress. In addition, we also determined the long-time salt stress tolerance of the potted plants. When 1-month-old plants were subjected to 200 mM NaCl for 14 d, the WTt exhibited a more serious wilting or necrosis compared with the *RmNHX2* overexpressing lines (Fig. 4d). Consistent with the enhanced salt tolerance

phenotype, the content of EL and MDA in the transgenic lines was significantly lower than in the WTt after salt stress (Fig. 4e, f), indicating that cellular damage was more serious in the WTt. Furthermore, higher Chl level in transgenic lines compared with WTt was observed (Fig. 4g). The mentioned results demonstrated that *RmNHX2* overexpression could increase the salt tolerance of transgenic tobacco.

Silencing of *RmNHX2 in Rosa multiflora* conferred sensitivity to salt stress

To elucidate the function of *RmNHX2 in salt tolerance, the VIGS system was conducted to silence RmNHX2* expression in *Rosa multiflora*. The transcript level of *RmNHX2 in the VIGS plants was down-regulated by 30-60% in comparison with that of the empty vector (pTRV2) transformed control plants (WTr) (Supplementary Fig. 4). We further assessed the salt tolerance of the mentioned two pTRV2-RmNHX2* VIGS plants (designated as pTRV2-1 and pTRV2-2) exposed to salt stress. First, both pTRV2-*RmNHX2* VIGS and WTr plants grown in hydroponic solution were exposed to 300 mM NaCl for 7 d. After the salt treatment, the VIGS lines showed more severe wilting phenotypes in comparison with the WTr (Fig. 5a). In addition, EL and MDA, related to the cell damages, were determined. At the end of salt stress, the EL of pTRV2-1 (62.0 %) and pTRV2-2 (59.0 %) was significantly higher as compared with 46.4 % of WTr (Fig. 5b). Meanwhile, the pTRV2-1 and pTRV2-2 presented higher MDA relative to WTr after the salt stress (Fig. 5c). As shown in Fig. 5d, the total chlorophyll content of the *RmNHX2*-VIGS plants were nearly 2.0 folds lower than that of WTr under salt stress.

To gain insights into whether *RmNHX2* was associated with salt tolerance, the *RmNHX2*-VIGS plants and WTr were treated at 300 mM NaCl. No visible phenotypic differences were identified between the *RmNHX2*-VIGS plants and WTr without salt stress. After the salt treatment for 10 d, the pTRV2-1 and pTRV2-2 plants suggested more serious damage relative to the WTr plants (Fig. 5e). When the salt treatment was completed, the Chlorophyll extracting of WTr displayed paler in color than the *RmNHX2*-VIGS plants (Fig. 5f). Consistent with the observed phenotype, the EL and MDA in the *RmNHX2*-VIGS plants were prominently higher than as compared with those of the WTr, implying that the VIGS plants were damaged to greater degree (Fig. 5g, h). Furthermore, the pTRV2-1 and pTRV2-2 plants achieved significantly lower levels of total chlorophyll than those of WTr after salt stress (Fig. 5i). Taken together, the mentioned data suggested that silencing of *RmNHX2 in Rosa multiflora* led to the elevated the salt sensitivity.

Analysis of H_2O_2 and O_2^- in transgenic tobacco and *Rosa multiflora* silenced plants under salt stress

Abiotic stresses were extensively evidenced to often induce ROS accumulation, thereby causing serious oxidative damage. ROS accumulation refers to a major indicator of stress tolerance. To verify whether *RmNHX2* is closely associated with enhanced salt tolerance of plants via ROS scavenging, DAB and NBT were performed to detect H_2O_2 and O_2^- productions, respectively, in transgenic and wild-type plants after the salt stress. Under 30-day-old tobaccos grown in soil pots administrated with 200 mM NaCl for 14 d, the WTt leaf discs were stained deeper and more intensely by NBT and DAB in compared with the *RmNHX2*-overexpressing transgenic lines (Fig. 6a, b). In contrast to the mentioned, deeper DAB and NBT

staining were visualized in pTRV2-*RmNHX2* plants in contrast to the control plants (Fig. 6c, d), implying that ROS accumulation was enhanced when *RmNHX2* was silenced. For the verification of DAB and NBT staining results, the authors determined the H_2O_2 and O_2^- levels in the salt-treated leaves as well. Consistent with the staining, the levels of H_2O_2 and O_2^- were significantly lower in the transgenic tobacco lines compared with WTt, as indicated by the measured results (Fig. 6e, f). In contrast, the pTRV2-*RmNHX2* VIGS plants accumulated more ROS than did WTr (Fig. 6g, h). Both results suggested that the *RmNHX2* overexpression led to the lower ROS accumulation in comparison with the WTt after salt treatment, whereas they also showed in an opposite way when *RmNHX2* was down-regulated.

Analysis of antioxidant enzyme activities and expression levels of the encoding genes in transgenic tobacco and *Rosa multiflora* silenced plants under salt stress

Antioxidant enzymes positively impact ROS scavenging under abiotic stresses, which impelled us to assess the CAT, POD and SOD enzyme activities (Gill and Tuteja, 2010). When the 30-day-old potted tobacco plants were exposed to the salt treatment for 14 d, the activities of the CAT, POD and SOD in the transgenic plants were significantly higher than those in the WTt (Fig. 7a-c). Furthermore, the expression levels of CAT, POD and SOD in *RmNHX2* overexpression tobacco plants were significantly up-regulated compared with that in the WTt after salt treatment (Fig. 7d-f). In contrast to the mentioned, noticeably lower three enzyme activities were observed in the two VIGS plants (pTRV2-1 and pTRV2-2) than in the WTr plants at the end of salt stress (Fig. 7g-i). However, it was displayed opposite way when the *RmNHX2* expression was down-regulated (Fig. 7j-l). The mentioned finding suggested that *RmNHX2* functioned in salt tolerance, at least partially, resulted from the increased actions of CAT, POD and SOD.

Opposite accumulation of Na^+ and K^+ in transgenic tobacco and *Rosa multiflora* silenced plants under salt stress

Plant's Na^+ balance is considered disrupted under salt stress. Given that overexpression or down-regulation of *RmNHX2* influenced the salt tolerance of plants, we were urged to assess whether ionic homeostasis was affected under salt stress. To tackle down the mentioned issues, we also measured the content of Na^+ and K^+ in the leaves and roots. Upon exposure to salt stress, the Na^+ levels were 11.91 mg/g dry weight (DW) in WTt tobacco roots, 7.38 mg/g DW in OE1, 8.76 mg/g DW in OE7 and 9.63 mg/g DW in OE9 (Fig. 8a). The leaves Na^+ levels were lower in the OE1, OE7 and OE9 as compared with those in the WTt (Fig. 8b). Moreover, the leave and the root in the *RmNHX2* overexpression tobacco plants accumulated more K^+ than those in the WTt leaves and roots (Fig. 8b). As a result, the Na/K ratios in WTt were noticeably higher than in the transgenic tobacco lines after salt treatment (Fig. 8c). Conversely, the levels of Na^+, K^+ and Na/K in the two pTRV2-*RmNHX2* VIGS lines were significantly higher or lower than those of the WTr plants after salt stress, respectively (Fig. 8d-f). The mentioned data demonstrated that the enhanced tolerance of transgenic tobacco lines and susceptibility of pTRV2-*RmNHX2* VIGS plants to salt stress were closely related to ion homeostasis.

Discussion

Previous studies have shown that plant intracellular Na^+/H^+ antiporters play significant roles in adaption to salt stress through the maintenance of cellular PH and ionic equilibrium (Guan et al. 2011; Xu et al. 2010). Though several NHXs have been described in the model plants, e.g., *Arabidopsis thaliana*, rice and cotton, knowledge is still limited concerning the function and action mechanism of plant NHXs in perennial woody ornamental plants. Thus, clarifying NHXs function in perennial plants, e.g., *Rosa multiflora*, will provide a better understanding on the role of NHXs.

In this study, we confirmed 11 RmNHXs proteins in *Rosa multiflora* through the genome-wide analysis. Most of the *RmNHXs* are responsive to salt stress, of which *RmNHX2* was particularly elevated. As revealed from multiple sequences alignment of RmNHX2 and other plants NHXs, RmNHX2 contained twelve transmembrane domains and amiloride binding motif in the N-terminal. Thus, RmNHX2 could be clustered into the typical NHX group. The phylogenetic analysis indicated that RmNHX2 pertained to the vacuolar Na^+/H^+ antiporter proteins and displayed closer associations with FvNHX2.

A number of studies had presented data suggesting that one of the main features of plants NHXs was up-regulation of their transcript level by salt stress (Gouiaa et al. 2012, Pandey et al. 2016). In the present study, salt treatment could up-regulate *RmNHX2*. It should be pointed out that the salt treatment is rather dramatic. Accordingly, more moderate stress treatments are required to do in-depth work and elucidate the gene expression pattern, as an attempt to extend results to the practical situations. As to expectation, *RmNHX2* overexpression also enhanced the salt tolerance in tobacco, as revealed by lower MDA and EL contents than the WTt, which was consistent with previous reports (Li et al. 2013, Li et al. 2010). MDA and EL are two key indicators of lipid peroxidation, displaying a close relationship to the membrane systems (Geng et al. 2020). Thus, it is normally proposed that the *RmNHX2* overexpression lines experienced lower degree of membrane injuries in comparison with WTt when exposed to salt stress. On the whole, environmental stress led to the excessive accumulation of ROS as well (e.g., H_2O_2 and O_2^-), thereby probably inducing the lipid peroxidation. Thus, ROS forming and concentration pattern were usually used as a key indicator to evaluate the stress tolerance (Gill et al. 2010; Geng and Liu 2018). Of special note, the transgenic tobacco lines accumulated significantly less H_2O_2 and O_2^- than WTt by DAB and NBT staining, suggesting that transgenic plants suffered from milder salt stresses, which agreed with the measured data of MDA and EL. Based on the mentioned evidence, we assumed that the lower concentration of ROS in *RmNHX2* transgenic lines constitutes a physiological mechanism partly; if not fully, underlying *RmNHX2* mediated salt tolerance in the overexpression lines.

This is further supported by concurrent observation of an elevation of ROS contents and increased salt sensibility in the VIGS lines with silencing of *RmNHX2*. ROS accumulation under stress condition displays a tight association with the equilibrium between ROS accumulation and scavenging (Miller et al. 2010). ROS-scavenging enzymes (e.g., SOD, CAT and POD) positively impacted ROS detoxification to alleviate cell damage under environmental stresses (Pitzschke et al. 2009). In subsequent experiments, the SOD, POD, and CAT activities noticeably increased in transgenic line as compared with those of the WTt under

the salt stress. The greater enzyme activities may account for the accumulation of less ROS in the mentioned lines. However, the expression levels of antioxidant genes were significantly down-regulated in *RmNHX2*-VIGS lines, which complied with the higher contents of ROS. This study demonstrated that *RmNHX2* functions in salt tolerance through a more powerful ROS-scavenging capacity.

It is conceivable that excessive cytosolic Na^+ accumulation in plant cell induced cell injury and ionic toxicity as well, thereby resulting in ion imbalance and perturbation of Na : K ratio (Yang et al. 2017; Zhang et al. 2017). In addition, the level of K^+ in cellular also affects the salt tolerance of plants (Xiong et al. 2002). In the present study, the *RmNHX2* overexpression tobacco lines showed the enhanced tolerance of salt with lower Na^+ level, but with higher concentrations of K^+ and reduced Na/K ratios, whereas salt sensitivity of the *RmNHX2* VIGS lines is consistent with higher Na^+ level, reduced K^+ and increased Na/K ratio. Thus, the enhanced salt tolerance of *RmNHX2* overexpression tobacco lines might be ascribed to the efficient maintenance of ion balance.

Conclusion

In this study, we confirmed 11 RmNHXs proteins in *Rosa multiflora* through the genome-wide analysis. Most of the *RmNHXs* are responsive to salt stress, of which RmNHX2 was particularly elevated. RmNHX2 was localized at the tonoplast. *RmNHX2* overexpression in tobacco led to the increased tolerance to salt, while silencing of *RmNHX2* in *Rosa multiflora* increased salt susceptibility. *RmNHX2*-mediated salt tolerance might be at least in part via the antioxidant system and ion homeostasis (Fig. 9). Accordingly, *RmNHX2*, as an important candidate gene, had a great potential for molecular breeding of salt-tolerant woody ornamental plants.

Abbreviations

NHX, Na^+/H^+exchanger; VIGS, Virus-induced gene silencing; ROS, reactive oxygen species; EL, Electrolyte leakage; MDA, malondialdehyde; DAB, 3,3’ diaminobenzidine; NBT, nitro blue tetrazolium; HMM, Hidden Markov Model; Mw, molecular weight; pI, isoelectric point;

Declarations

Funding This work was supported by grants from the National Natural Science Foundation of China (No. 31800598 and No. 32171851), the Fundamental Research Funds for the Zhejiang A&F University (No. 2016FR033) and the National Key R&D Program of China (No. 2018YFD1000404).

Conflicts of interest The authors declare that they have no competing interests.

Data availability and material The datasets generated during and/or analyzed during the current study are available from the corresponding author on reasonable request.

Code availability Not applicable for that section.

Author contributions PL conceived the study and participated in its design. PL, YXS, LMC and WC performed experiments. PL and YYC analyzed the data and wrote the manuscript. All authors have read and approved the manuscript.

References

1. Banjara M, Zhu LF, Shen GX et al (2012) Expression of an *Arabidopsis* sodium/proton antiporter gene (*AtNHX1*) in peanut to improve salt tolerance. *Plant Bio Re* 6: 59-67.
2. Bai L, Ma X, Zhang G et al (2014) A receptor-like kinase mediates ammonium homeostasis and is important for the polar growth of root hairs in *Arabidopsis*. *Plant Cell* 26: 1497-1511.
3. Bassil E, Blumwald E (2014) The ins and outs of intracellular ion homeostasis: NHX type cation/H+ transporters. *Curr Opin Plant Biol* 22: 1-6.
4. Bassil E, Tajima H, Liang Y et al (2011) The *Arabidopsis* Na^+/H^+ antiporters NHX1 and NHX2 control vacuolar pH and K^+ homeostasis to regulate growth, flower development, and reproduction. *Plant Cell* 23: 3482-3497.
5. Chen C, Chen H, He Y et al (2020) TBtools: An integrative toolkit developed for interactive analyses of big biological data. Mol Plant 8: 1194-1202.
6. Dong W, Wang MC, Xu F et al (2013) Wheat oxophytodienoate reductase gene *TaOPR1* confers salinity tolerance via enhancement of abscisic acid signaling and reactive oxygen species scavenging. *Plant Physiol* 161: 1217-1228.
7. Deinlein U, Stephan AB, Horie T et al (2014) Plant salt-tolerance mechanisms. *Trends in Plant Sci* 19: 371-379.
8. Dong HZ, Wang CM, Xing CH et al (2019) Overexpression of *PbrNHX2* gene, a Na^+/H^+ antiporter gene isolated from *Pyrus betulaefolia*, confers enhanced tolerance to salt stress via modulating ROS levels. *Plant Sci* 285:14-25.
9. Dahro B, Wang F, Peng T et al (2016) PtrA/NINV, an alkaline/neutral invertase gene of *Poncirus trifoliata*, confers enhanced tolerance to multiple abiotic stresses by modulating ROS levels and maintaining photosynthetic efficiency. *BMC Plant Biol* 16: 76.
10. Giraud E, Aken OV, Ho LHM et al (2009) The transcription factor ABI4 is a regulator of mitochondrial retrograde expression of *Alternative oxidase. Plant Physiol* 150: 1286-1296.
11. Guan B, Hu YZ, Zeng Y et al (2011) Molecular characterization and functional analysis of a vacuolar Na^+/H^+ antiporter gene (*HcNHX1*) from *Halostachys caspica*. *Mol Biol Rep* 38: 1889-1899.
12. Gouiaa S, Khoudi H, Leidi EO et al (2012) Expression of wheat Na^+/H^+ antiporter *TNHXS1* and H^+-pyrophosphatase *TVP1* genes in tobacco from a bicistronic transcriptional unit improves salt tolerance. *Plant Mol Biol* 79: 137-155.
13. Geng JJ, Wei TL, Wang Y et al (2020) Overexpression of *PtrbHLH*, a basic helix-loop-helix transcription factor from *Poncirus trifoliata*, confers enhanced cold tolerance in pummelo (*Citrus grandis*) by modulation of H_2O_2 level via regulating a CAT gene. *Tree Physiol* 39: 2045-2054.

14. Gill SS, Tuteja N (2010) Reactive oxygen species and antioxidant machinery in abiotic stress tolerance in crop plants. *Plant Physiol Biol* 48: 909-930.
15. Geng JJ, Liu JH (2018) The transcription factor CsbHLH18 of sweet orange functions in modulation of cold tolerance and homeostasis of reactive oxygen species by regulating the antioxidant gene. *J Exp Bot* 69: 2677-2692.
16. Kronzucker HJ, Britto DT (2011) Sodium transport in plants: a critical review. *New Phytol* 189: 54-81.
17. Khaskheli AJ, Ahmed W, Ma C et al (2018) *RhERF113* functions in ethylene-induced petal senescence by modulating cytokinin content in rose. *Plant Cell Physiol* 59: 2442-2451.
18. Li C, Wei ZW, Liang D et al (2013) Enhanced salt resistance in apple plants overexpressing a *Malus* vacuolar Na^+/H^+ antiporter gene is associated with differences in stomatal behavior and photosynthesis. *Plant Physiol Bio* 70: 164-173.
19. Li YH, Zhang YZ, Feng FJ et al (2010) Overexpression of a *Malus* vacuolar Na^+/H^+ antiporter gene (*MdNHX1*) in apple rootstock M.26 and its influence on salt tolerance. *Plant Cell Tiss Org* 102: 337-345.
20. Livak KJ, Schmittgen TD (2002) Analysis of relative gene expression data using real-time quantitative PCR and the $2^{-\Delta\Delta ct}$ method. *Methods* 25: 402-408.
21. Li ZY, ChenW, Zhang C et al (2019) *RcMYBPA2* of *Rosa chinensis* functions in proanthocyanidin biosynthesis and enhances abiotic stress tolerance in transgenic tobacco. *Plant Cell Tiss Org* 137: 441-454.
22. Liu JH, Inoue H, Moriguchi T (2008) Salt stress-mediated changes in free polyamine titers and expression of genes responsible for polyamine biosynthesis of apple in vitro shoots. *Environ Exp Bot* 62: 28-35.
23. Luo P, Li ZY, Chen W et al (2020) Overexpression of *RmICE1*, a bHLH transcription factor from *Rosa multiflora*, enhances cold tolerance via modulating ROS levels and activating the expression of stress-responsive genes. *Environ Exp Bot* 178: 104160.
24. Mahajan S, Tuteja N (2005) Cold, salinity and drought stresses: an overview. *Arch Biochem Biophys* 444: 139-158.
25. Miller G, Suzuki N, Ciftci-Yilmaz S et al (2010). Reactive oxygen species homeostasis and signalling during drought and salinity stresses. *Plant Cell Environ* 33: 453-467
26. Ma XN, Zhang XR, Yang L et al (2019) Hydrogen peroxide plays an important role in PERK4-mediated abscisic acid-regulated root growth in *Arabidopsis*. *Funct Plant Biol* 46: 165-174.
27. Phukan U J, Jeena GS, Tripathi V et al (2017) MaRAP2-4, a waterlogging-responsive ERF from Mentha, regulates bidirectional sugar transporter AtSWEET10 to modulate stress response in *Arabidopsis*. *Plant Biotechnol J* 16: 221-233.
28. Pandey S, Patel MK, Mishra A et al (2016) In planta transformed cumin (*Cuminum cyminum* L.) plants, overexpressing the *SbNHX1* gene showed enhanced salt endurance. *Plos One* 11: e0159349.

29. Pitzschke A, Djamei A, Bitton F et al (2009) A major role of the MEKK1-MKK1/2-MPK4 pathway in ROS signalling. *Mol Plant* 2: 120-137.
30. Qiao WH, Zhao XY, Li W et al (2007) Overexpression of *AeNHX1*, a root-specific vacuolar Na^+/H^+ antiporter from *Agropyron elongatum*, confers salt tolerance to *Arabidopsis* and *Festuca* plants. *Plant Cell Rep* 26: 1663-1672.
31. Teakle NL, Amtmann A, Real D et al (2010) Lotus tenuis tolerates combined salinity and waterlogging: maintaining O_2 transport to roots and expression of an NHX1-like gene contribute to regulation of Na^+ transport. *Physiol Plantarum* 139: 358-374
32. Tian J, Pei HX, Zhang S et al (2014) TRV-GFP: a modifed Tobacco rattle virus vector for effcient and visualizable analysis of gene function. *J Exp Bot* 65: 311-322
33. Wang M, Dai WS, Du J et al (2019) ERF109 of trifoliate orange (*Poncirus trifoliata* (L.) Raf.) contributes to cold tolerance by directly regulating expression of *Prx1* involved in antioxidative process. *Plant Biotechnol J* 17: 1316-1332.
34. Wu H, Fu B, Sun PP et al (2016) A NAC transcription factor represses putrescine biosynthesis and affects drought tolerance. *Plant Physiol* 172: 1532-1547.
35. Xu K, Zhang H, Blumwald E et al (2010) A novel plant vacuolar Na^+/H^+ antiporter gene evolved by DNA shuffling confers improved salt tolerance in yeast. *J Biol Chem* 285: 22999-23006.
36. Xiong LM, Schumaker KS, Zhu JK (2002) Cell signaling during cold, drought, and salt stress. *Plant Cell* 14: 65-83.
37. Yoshida T, Mogami J, Yamaguchi-Shinozaki K (2014) ABA-dependent and ABA-independent signaling in response to osmotic stress in plants. *Curr Opin Plant Biol* 21: 133-139.
38. Yu JL, Ge HM, Wang XK et al (2017) Overexpression of pyrabactin resistance-like abscisic acid receptors enhances drought, osmotic, and cold tolerance in transgenic poplars. *Front Plant Sci* 8: 1752.
39. Yuan HJ, Ma Q, Wu GQ et al (2015) *ZxNHX* controls Na^+ and K^+ homeostasis at the whole-plant level in *Zygophyllum xanthoxylum* through feedback regulation of the expression of genes involved in their transport. *Ann Bot* 115: 495-507.
40. Yang YQ, Yan G (2017) Elucidating the molecular mechanisms mediating plant salt: tress responses. *New Phytol* 217: 523-539.
41. Zhu JK (2002) Salt and drought stress signal transduction in plants. *Annu Rev Plant Biol* 53: 247-273.
42. Zhang XM, Cheng ZH, Zhao K et al (2019) Functional characterization of poplar *NAC13* gene in salt tolerance. *Plant Sci* 281: 1-8.
43. Zhang YM, Zhang HM, Liu ZH et al (2015) The wheat NHX antiporter gene *TaNHX2* confers salt tolerance in transgenic alfalfa by increasing the retention capacity of intracellular potassium. *Plant Mol Biol* 87: 317-327.

44. Zeng Y, Li Q, Wang H et al (2018) Two NHX-type transporters from *Helianthus tuberosus* improve the tolerance of rice to salinity and nutrient deficiency stress. *Plant Biotechnol J* 6: 310-321.
45. Zhang WW, Meng JJ, Xing JY et al (2017) The K^+/H^+ antiporter AhNHX1 improved tobacco tolerance to NaCl stress by enhancing K^+ retention. *J Plant Biol* 60: 259-267.
46. Zhang M, Zhang GQ, Kang HH et al (2017) *TaPUB1*, a putative E3 ligase gene from wheat, enhances salt stress tolerance in transgenic *Nicotiana benthamiana*. *Plant Cell Physiol* 58: 1673-1688.

Figures

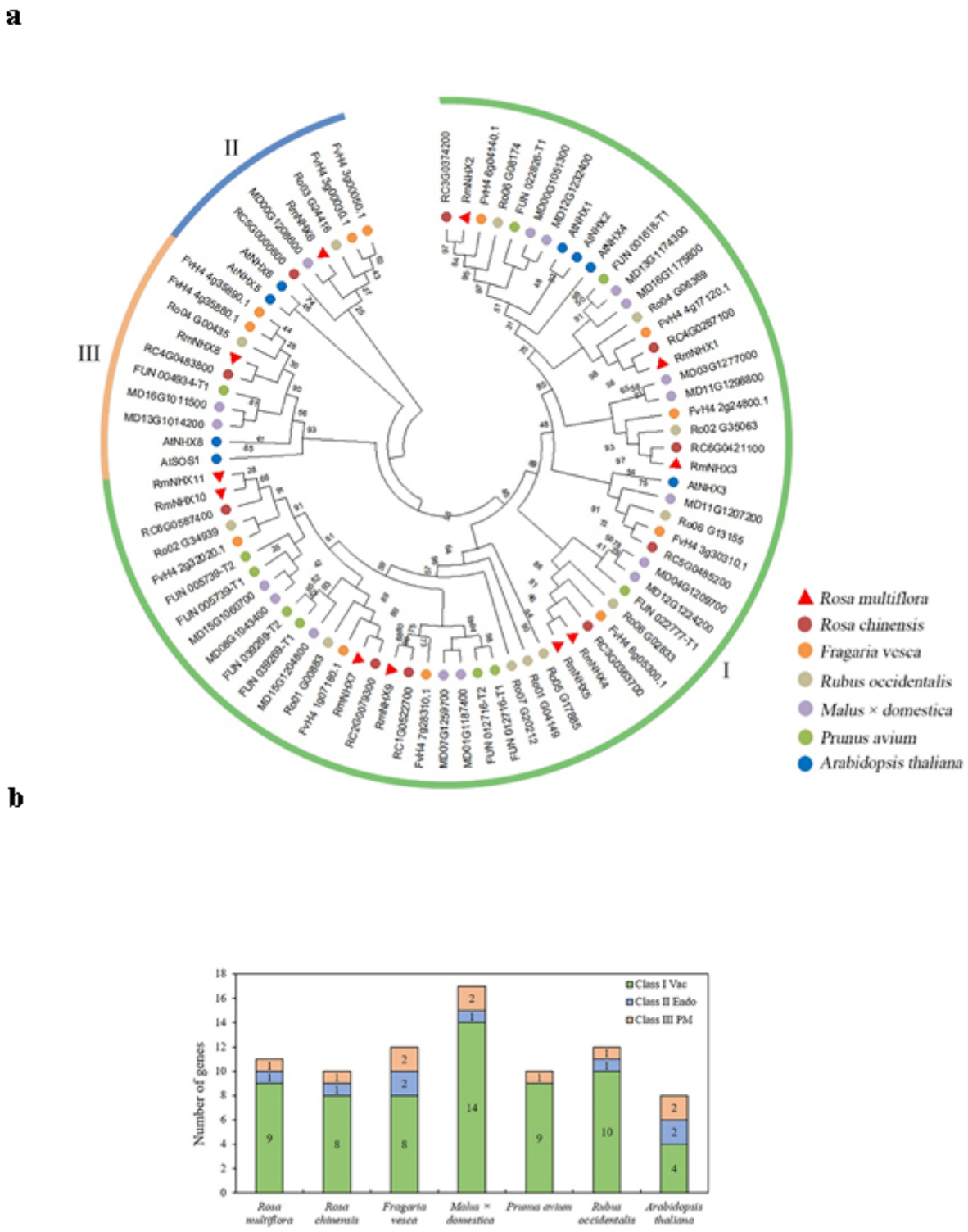

Figure 1

Phylogenetic tree analysis of NHX gene family. a Phylogenetic clustering of from wild rose, rosa, strawberry, apple, cherry, raspberry and Arabidopsis. MEGA 7 was used to construct the phylogenetic tree with the NJ method. The proteins were clustered into 3 groups. Different background colors indicate the different group of the NHXs proteins. b the number of three types NHX gene in wild rose, rosa, strawberry, apple, cherry, raspberry and Arabidopsis.

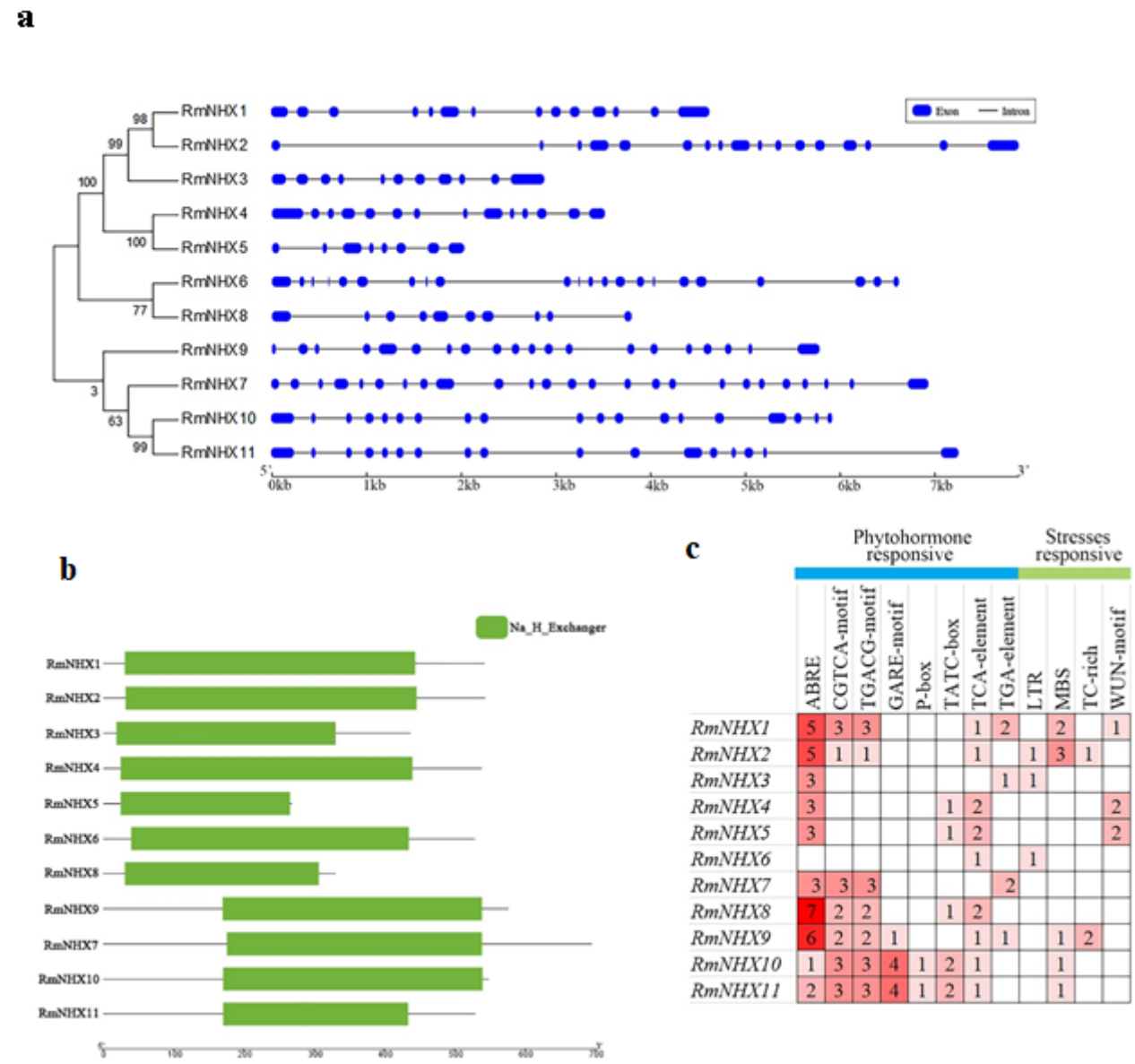

Figure 2

The conserved motifs and gene structure analysis of RmNHX genes family in wild rose. a Gene structure analysis of RmNHXs. Exons are represented by boxes, while introns are represented by gray lines. The cis-acting elements are indicated in diferent colored boxes. b Conserved motif analysis of RmNHXs. Na+/H+ exchanger domain is marked in green. c Promoter analysis of cis-acting regulatory elements related to stress response in RmNHXs.

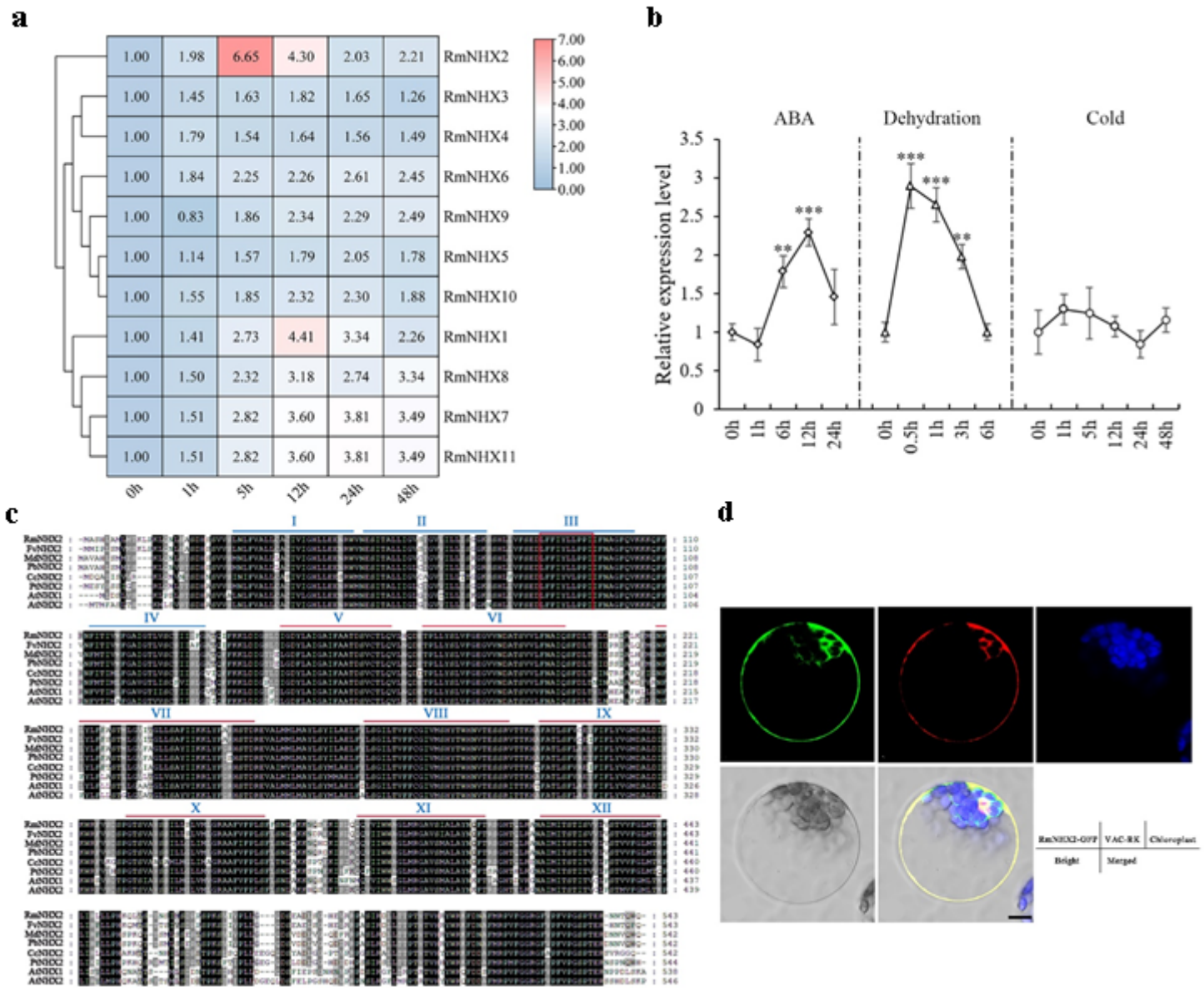

Figure 3

Time-course expression levels of RmNHX genes in Rosa multiflora under abiotic stress and subcellular localization analysis of RmNHX2. a Heatmap analysis of RmNHX genes in response to salt stress. b RmNHX2 expression levels in R.multiflora exposed to cold, dehydration and ABA. RmGAPDH was used as an reference gene. The expression level at time point 0 was defined as 1.0 and data represented means ± SE of three replicates. c Amino acid sequence alignment of RmNHX2 and other NHXs from other plants. Identical amino acids are shown with a black background and analogous amino acids are shaded in gray. The 12 transmembrane domains typical for a vacuolar-type Na+/H+ antiporter were shown by lines. The accession numbers of these known proteins in GenBank are: FvNHX2, XP_004289614.1; MdNHX2, XP_028954695.1; PbNHX2, XP_009352430.1; CcNHX2, XP_006433113.1; PtNHX2, XP_002307194.2; AtNHX1, NP_198067.1; AtNHX2, NP_001326210.1. d Arabidopsis protoplasts cells were transiently transformed with constructs containing fusion plasmid (RmNHX2: GFP) and tonoplast located marker

(VAC:RK). Colum a to e show GFP signals, VAC: RK signals, merged images of GFP and RFP signals, and bright-field. Bar = 10 μm. Three biological experiments were performed, which produced similar results.

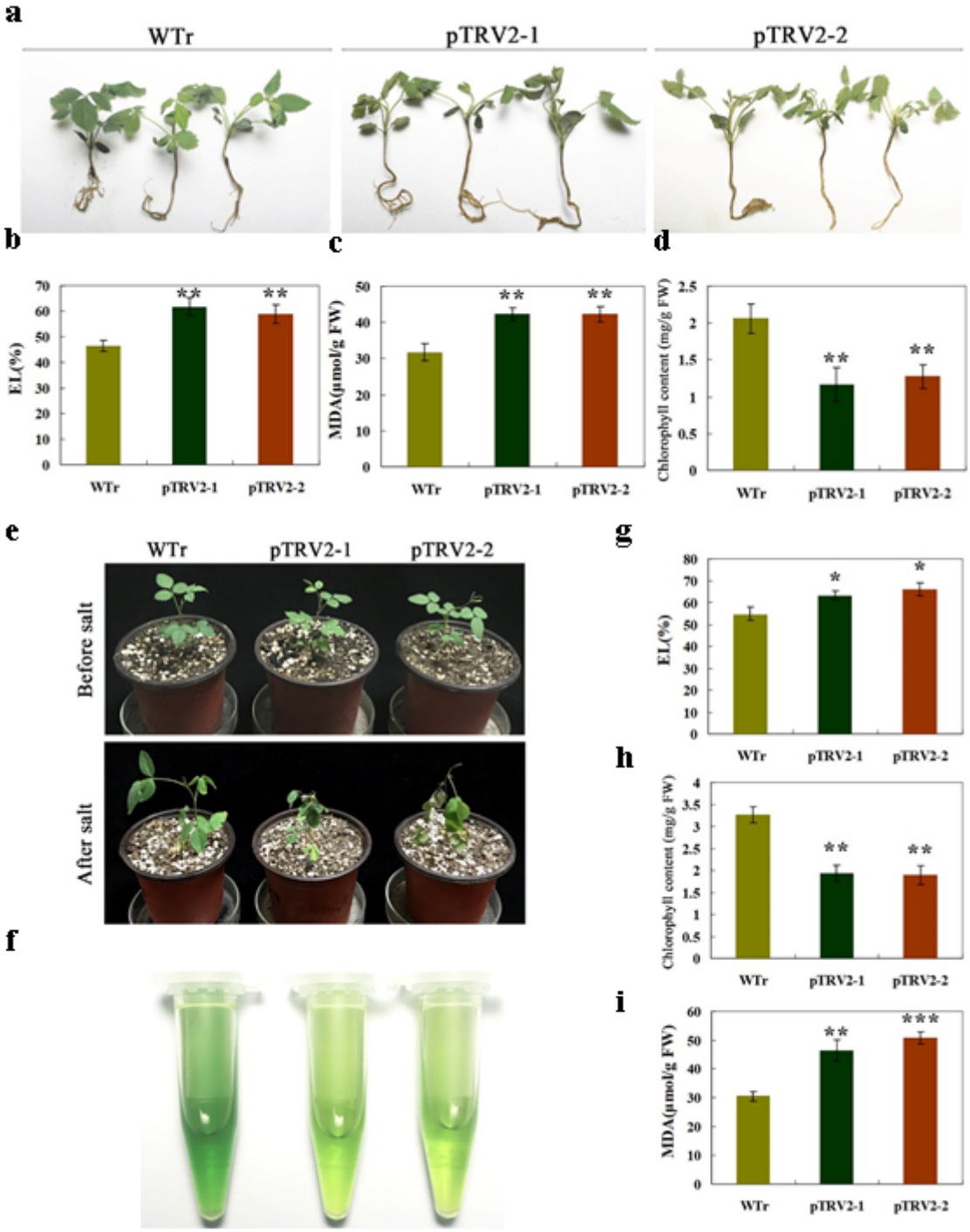

Figure 4

Overexpression of RmNHX2 conferred enhanced salt tolerance in tobacco. a Leaf morphology of WTt and transgenic tobacco lines before and after treatment with 200 mM NaCl for 24 h. b Electrolyte leakage of the WTt, OE-1, OE-7 and OE-9 after 200 mM NaCl treatment for 24 h. c MDA levels of WTt, OE-1, OE-7 and OE-9 after 200 mM NaCl treatment for 24 h. d Phenotypes of 30-day-old plants of transgenic lines (OE-1, OE-7 and OE-9) and WTt before and after 200 mM NaCl salt stress for 14 d. e-g Electrolyte leakage (e),

MDA (f) and chlorophyll contents (g) of the WTt, OE-1, OE-7 and OE-9 after 200 mM NaCl salt stress for 14 d. Error bars represent ± SE (n=3). Asterisks indicate significant differences between transgenic lines and WT (*P < 0.05, **P < 0.01, ***P < 0.001).

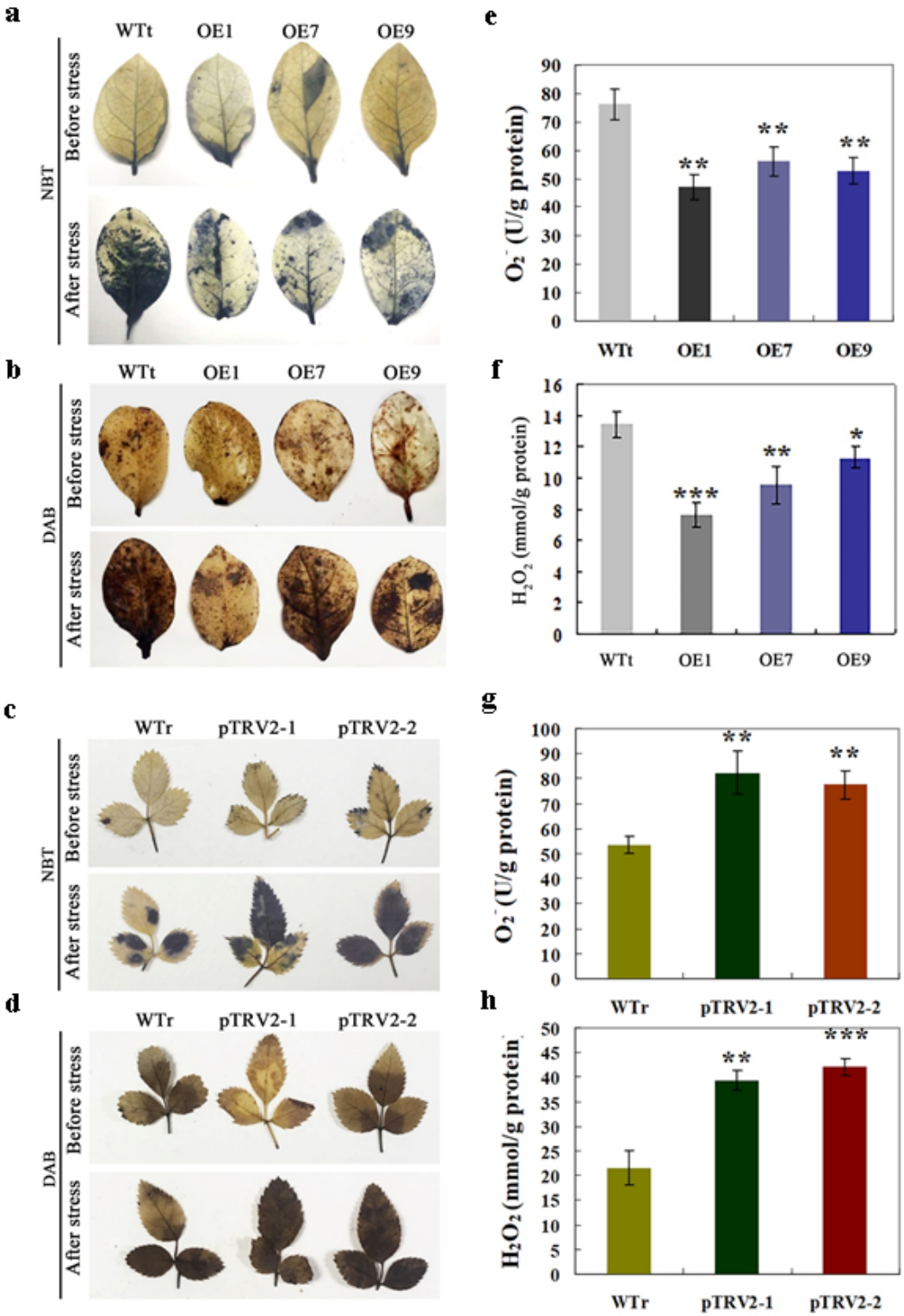

Figure 5

Silencing of RmNHX2 led to enhanced salt sensitivity in R.multiflora. a Phenotypes of 15 d VIGS plants (pTRV2-1 and pTRV2-2 and wild rose (WTr) after salt treatment (300 mM NaCl for 7 d). b-d EL (b), MDA

(c) and Chlorophyll contents (d) of VIGS plants and WTr after the 7 d salt treatment. e Phenotypes of 30 d VIGS potted plants and wild rose (WTr) before and after salt treatment (300 mM NaCl for 14 d). f The chlorophyll extraction solutions of RmNHX2-silenced plants at the end of salt stress. g-i EL (g), MDA (h) and chlorophyll contents (i) of VIGS plants and WTr after the 14 d 300 mM NaCl treatment. Error bars represent ± SE (n=3). Asterisks indicate significant differences between transgenic lines and WT (*P < 0.05, **P < 0.01, ***P < 0.001).

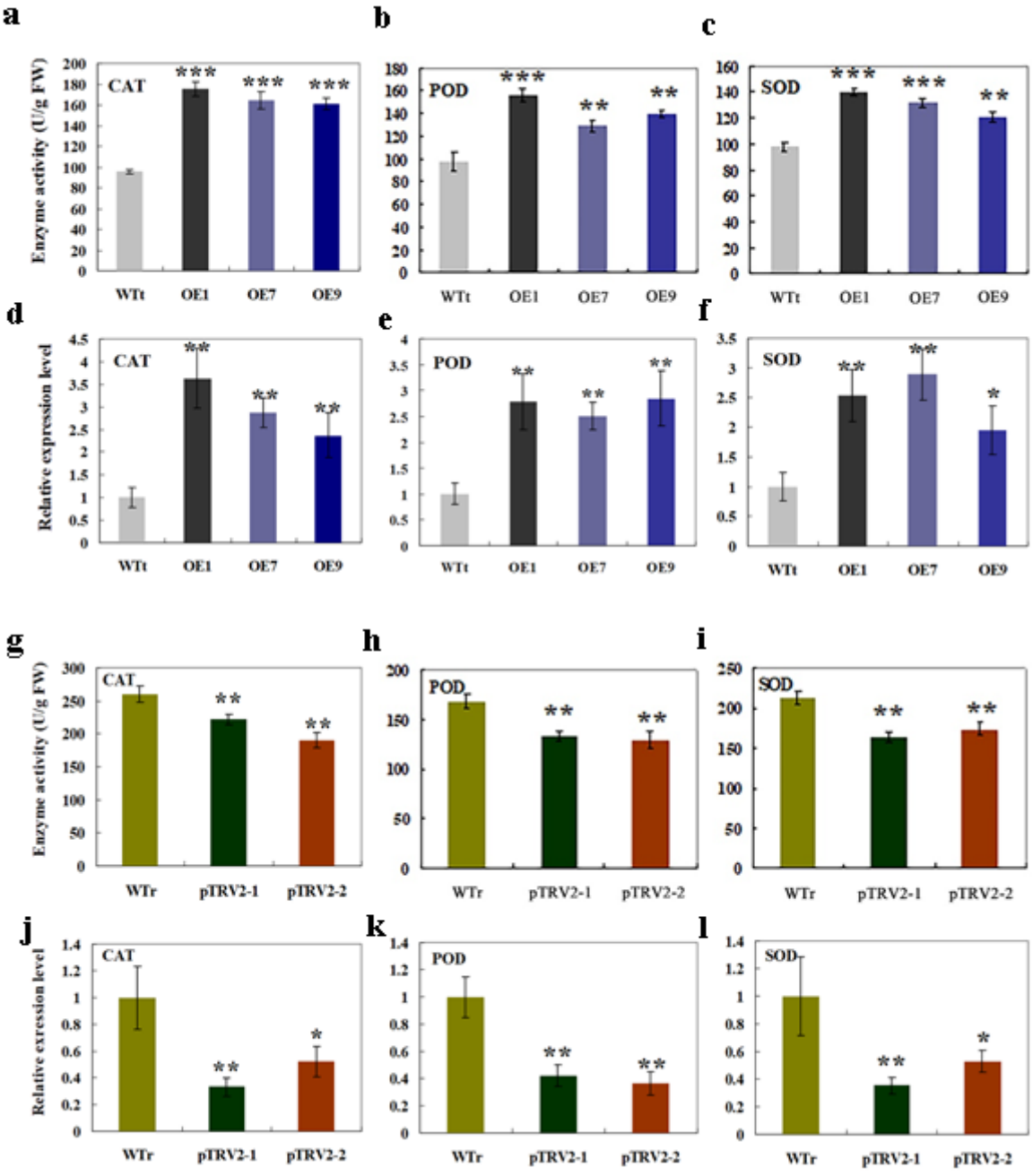

Figure 6

Analysis of O2- and H2O2 in transgenic tobacco and R.multiflora silenced plants after salt stresses. a Histochemical staining with NBT for detection of O2- in WTt, OE-1, OE-7 and OE-9 before and after 14 d of 200 mM NaCl. b Histochemical staining with DAB for detection of H2O2 in WTt, OE-1, OE-7 and OE-9

before and after 14 d of 200 mM NaCl. c Representative photos showing accumulation of O2- in WTr and wild rose silenced plants before and after 14 d of 300 mM NaCl. d Representative photos showing accumulation of H2O2 in WTr and wild rose silenced plants before and after 14 d of 300 mM NaCl. e-f Levels of O2- (e) and H2O2 (f) in tobacco WTt and transgenic lines (OE-1, OE-7 and OE-9) after 14 d of 200 mM NaCl stress. g-h Levels of O2- (g) and H2O2 (h) in wild rose WTr and silenced plants (pTRV2-1 and pTRV2-2) after 14 d of 300 mM NaCl stress. Error bars represent ± SE (n=3). Asterisks indicate significant differences between transgenic lines and WT (*P < 0.05, **P < 0.01, ***P < 0.001).

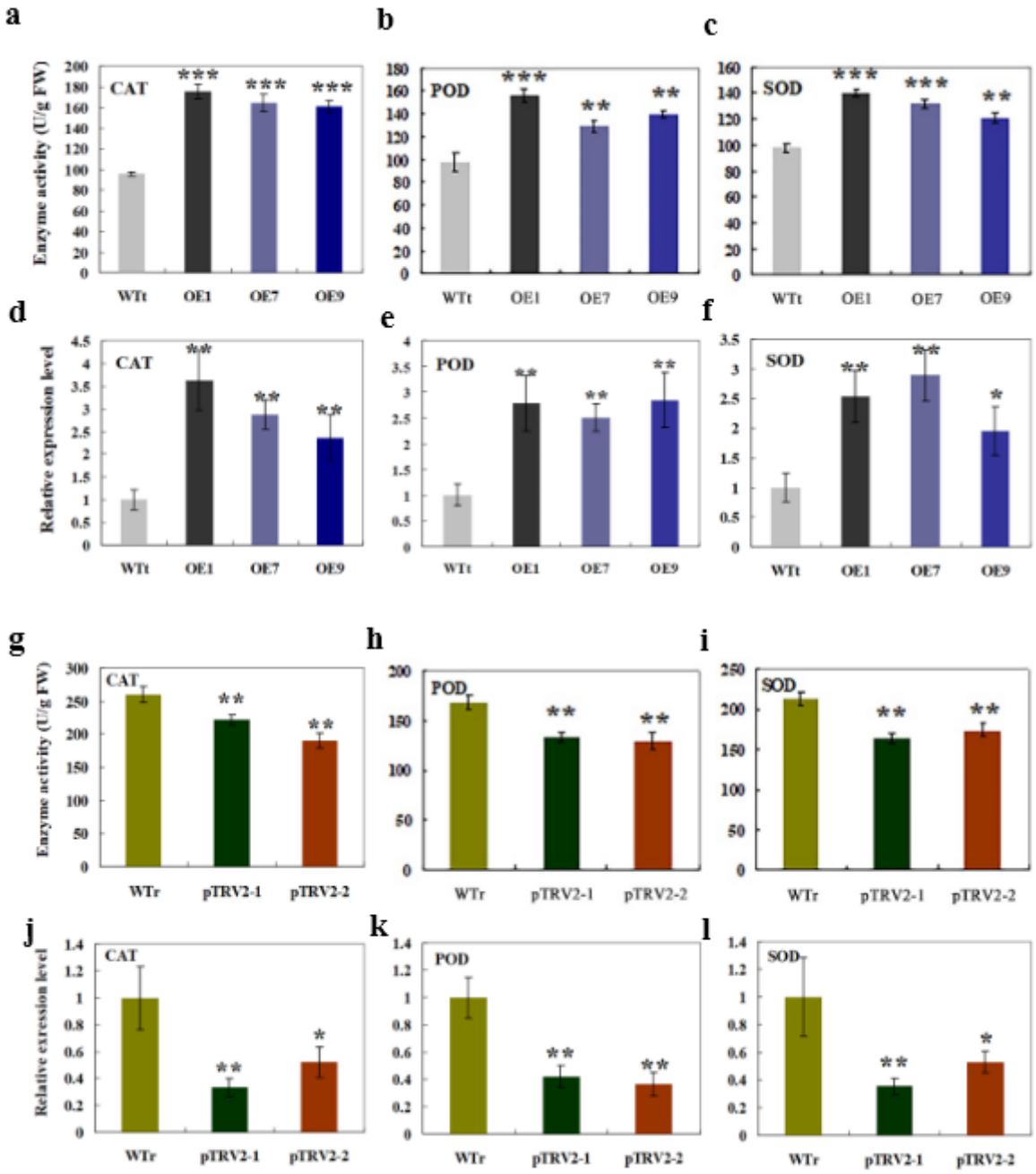

Figure 7

Analysis of enzyme activities and gene expression level related to antioxidant enzymes in tobacco and Rosa multiflora pTRV-RmNHX2 silenced plants after salt stress. a-c The activities of CAT (a), POD (b) and

SOD (c) in the WTt and transgenic tobacco plants after 14 d of 200 mM NaCl treatment. d-f The expression level of CAT (d), POD (e) and SOD (f) in the WTt and transgenic tobacco plants after 14 d of 200 mM NaCl treatment. g-i The activities of CAT (g), POD (h) and SOD (i) in the WTr and Rosa multiflora pTRV-RmNHX2 silenced plants after 14 d of 300 mM NaCl treatment. j-l The expression of CAT (j), POD (k) and SOD (l) in the WTr and Rosa multiflora pTRV2-RmNHX2 silenced plants after 14 d of 300 mM NaCl treatment. Error bars represent ± SE (n=3). Asterisks indicate significant differences between transgenic lines and WT (*P < 0.05, **P < 0.01, ***P < 0.001).

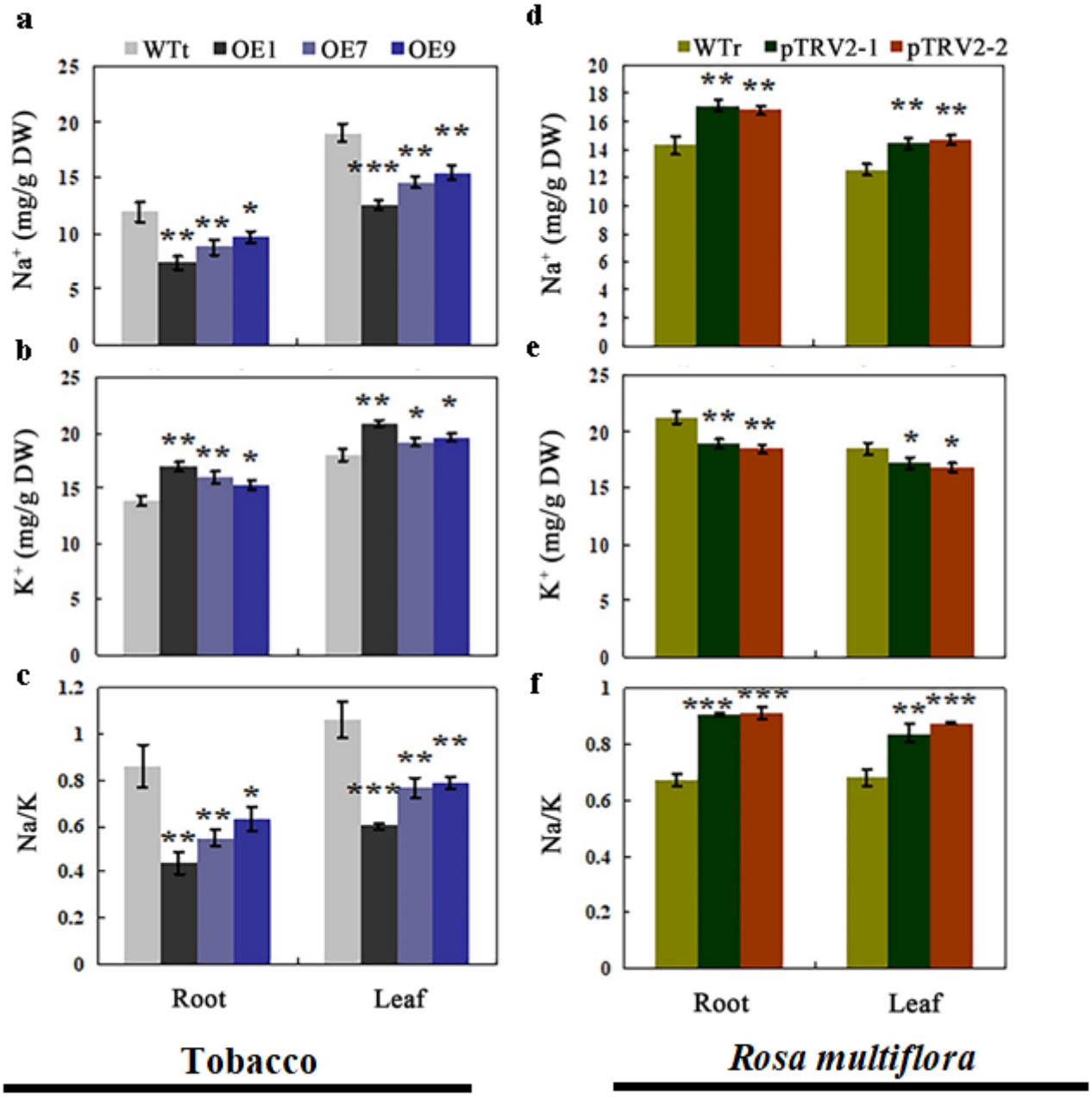

Figure 8

Ion levels in the leaves and roots of tobacco and Rosa multiflora pTRV2-RmNHX2 silenced plants. a-c The contents of Na+ (a), K+ (b) and the Na/K ratio (c) in the WTt and transgenic tobacco plants after 14 d of 200 mM NaCl treatment. d-f The contents of Na+ (d), K+ (e) and the Na/K ratio (f) in the WTr and Rosa

multiflora pTRV2-RmNHX2 silenced plants after 14 d of 300 mM NaCl treatment. Error bars represent ± SE (n=3). Asterisks indicate significant differences between transgenic lines and WT (*P < 0.05, **P < 0.01, ***P < 0.001).

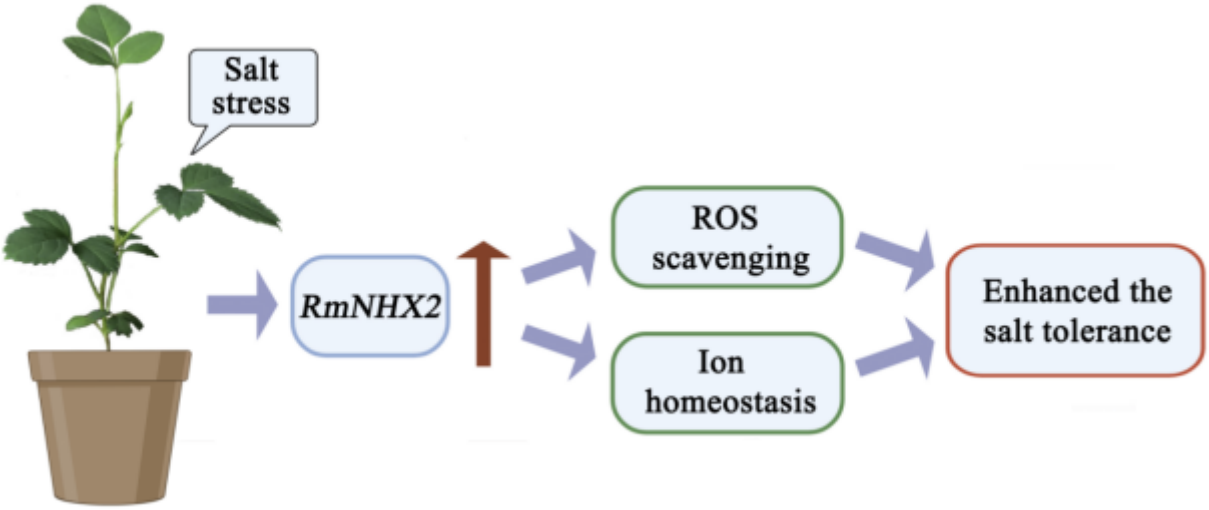

Figure 9

A proposed model of action for explaining regulatory function of RmNHX2 in response to salt stress. Salt stress could up-regulated the expression of RmNHX2 in Rosa multiflora. RmNHX2 enhances the salt tolerance via modulating the ROS scavenging system and ion homeostasis.

Supplementary Files

This is a list of supplementary files associated with this preprint. Click to download.

- Sup.doc